# Appendix A

# High-Dispersion Background Determination Algorithm (BCKGRD)

## A.1 Overview

The driving philosophy behind the NEWSIPS Project is to provide a homogeneous data product within a completely automated processing environment. An algorithm to compute background fluxes in high dispersion, *BCKGRD*, was designed with this philosophy. Although this algorithm generally provides a good background flux estimate, the results are not always optimal for particular regions of some images. A customized interactive determination of the background fluxes based on individual image characteristics can produce a more accurate estimate of the background in certain cases when data pathologies are present.

The determination of smoothed background fluxes follows the geometric resampling of pixels, so it is done with the high-dispersion resampled image (SI). A representative high-dispersion SI given in Figure A.1 shows echelle orders running horizontally and the spatial (cross-dispersion) direction running vertically. We will refer hereafter to the image sectors at the top and bottom as the "ends" of the image. The *BCKGRD* module produces smoothed background flux spectra which, together with the gross spectra, form the net spectra. The background model is created by computing continuous Chebyshev polynomial functions from pixels that sample valid background fluxes. For images with no continuum, the algorithm proceeds straightforwardly by sampling the neighboring interorder fluxes for each spectral order and fitting the result to a Chebyshev polynomial. The *BCKGRD* algorithm models the backgrounds of images having continuum flux in two one-dimensional passes, as described below.

For continuum source images, the background determination algorithm begins by sampling fluxes along the spatial direction with an extraction slit 5 pixels tall. We refer to these cuts as "swaths" and the steps taken for this group of vertical swaths as "Pass 1" operations. A total of 25 parallel swaths (26 for SWP) are taken in the spatial direction, each located at a column position ≈27 pixels larger than the preceding swath. Figure A.1 shows the positions of these Pass 1 swaths as dotted vertical lines. The mean flux is computed along the extraction slit from pixels containing valid local background fluxes; pixels are given a weight of zero if they fall along the spectral orders or if they do not contain valid fluxes (i.e., they have negative $\nu$ flags). The result of this process is a background-flux array for each swath that is discontinuous in spatial pixel number and contains noise. The array is adjusted to account for interorder contamination using a Point Spread Function (PSF) modeling technique described in Section A.2.2. The adjusted array is fit to a trial Chebyshev function of degree 7. This fitting degree is decreased if ringing is detected in the initial solution. The resulting solution is a smoothed continuous fit to the raw background fluxes. Each of the Pass 1 swaths is fit to a Chebyshev polynomial array in the same fashion.

In the second pass (Pass 2) solutions from Pass 1 are used to form a second and final set of 7th degree Chebyshev functions which model the background fluxes at the positions of the echelle orders. This solution is determined by sampling the solutions from the first pass at the locations where they intersect the echelle-order locations. The echelle-order locations are represented as solid lines in Figure A.1. The computation of a Chebyshev function from this sampling interpolates a continuous array of smoothed background fluxes at each wavelength along these orders. The solution is extrapolated beyond the target edges from the last calculated value.

The final background solutions are represented in two forms. First, a background vector of 768 values is saved and written to the high-dispersion merged extracted FITS file as a separate record for each order. Second, the 7 Chebyshev coefficients, together with a magnitude scale factor and starting and ending positions are written as FITS keywords. The "gross" spectrum may be reconstructed simply by adding the background and the net flux solutions.

## A.2 Background Determination: Step-by-Step

### A.2.1 Data Screening

Prior to the execution of the background determination algorithm, the fluxes and $\nu$ flags of each Pass 1 swath are evaluated to ensure that enough valid pixels exist in a swath to produce a reliable fit to the data. Any pixels containing flags with excessively negative ITF extrapolations or cosmic ray hits are added to a "pixels-to-avoid" working template for each Pass 1 swath. A few checks are then made to ensure that the background-determining algorithm will run properly. For example, if too few valid pixels can be found in a given Pass 1 swath to permit a reliable background extraction, the solution is set to a zero-flux array. If this is not repeated for the next swath, then the solution for the zeroed-out swath is reset to the mean of the two adjacent swaths.

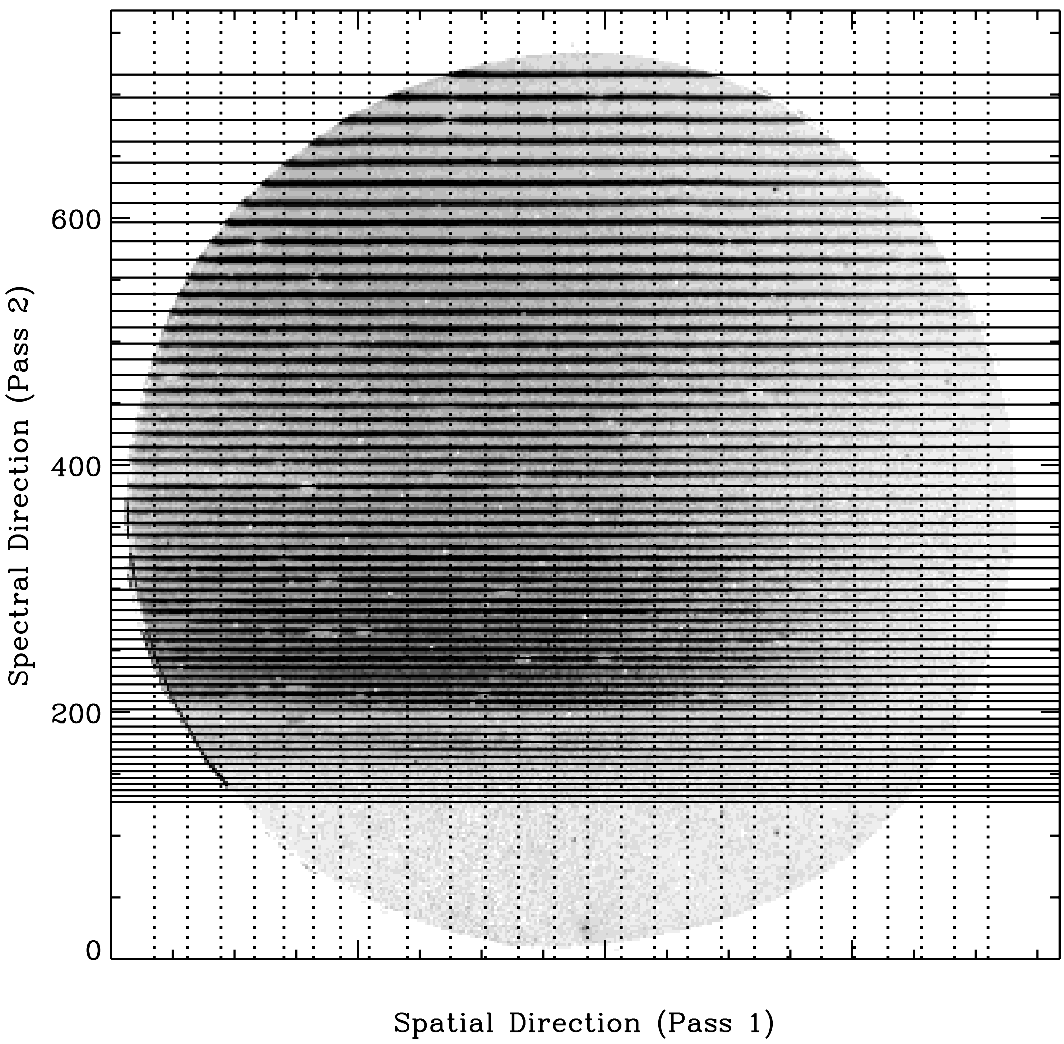


Figure A.1: Layout of the background extraction swaths on a sample SWP high-dispersion image. Lines running in vertical (spatial) direction are the Pass 1 extractions. Raw fluxes are sampled along these lines that are within the target ring and outside or between the echelle orders. The reconstructed background solutions created in Pass 2 are placed in the positions of the echelle orders (horizontal lines).

## A.2.2 Pass 1: Cross-Dispersion Swath Grid

### A.2.2.1 Basic Flow

For continuum source images, a series of 25 or 26 nearly equally spaced extraction swaths (slit height of 5 pixels) are made in the spatial direction of the high-dispersion SI, with a starting position at small spatial pixel numbers (short wavelength end). The swath sample positions were carefully selected to avoid contamination from any possible low-dispersion (double) exposure. Except for the first and last few Pass 1 swaths, which form short chords along the left and right edges of the camera image, each swath samples fluxes for nearly the entire range of sample positions; that is to say that they include pixels at the spatial ends of the camera which are not affected by contaminated interorder-overlap flux. The "interorder overlap" flux is described by a PSF model described below. The accumulated effects of overlapping PSFs increase as the orders become more closely spaced. The accumulation causes the interorder overlap to become increasingly severe until the camera sensitivity falls off at short wavelengths. It is this overlap which causes local background extractions in IUESIPS to be systematically high for short-wavelength orders and which necessitated a strategy for *BCKGRD* to sample background fluxes in distant uncontaminated regions as well as local contaminated ones.

The fluxes sampled from interorder pixels are modified if they are affected by contamination from neighboring orders. A model PSF provides an estimate of how much the fluxes should be offset before the Chebyshev fit is made (see "PSF Modeling" section below). The PSF model itself consists of two components, first, a monotonically decreasing function out to about four pixels and, second, a "halation ramp" which extends from four to about seven pixels from the center of each order profile. Each of these components is responsible for order overlap in a particular range of echelle orders. We will refer to the image area where the monotonic portion dominates as the "Interorder-Overlap Region" (IOR). The halation component is actually an extension of the IOR. However, *BCKGRD* treats it separately because, unlike the IOR, its characterization is independent of the order profiles.

The IOR and halation-dominated portions of the Pass 1 swath are indicated in Figure A.2. The initially sampled interorder fluxes in both the IOR and the halation regions are revised downward during the course of the calculations. The original and revised "working" fluxes are shown in this plot as squares and small crosses, respectively, and the flux revision for one point is shown as a downward pointing arrow. Fluxes for pixels in the halation-ramp region are affected by interorder contamination just like the triangle-inscribed IOR region, but in these cases only from the flat PSFs of the two neighboring orders. Because this overlap is constant, the algorithm may estimate it for several orders along the swath and determine a robust correction for halation. Note that the overwhelming majority of orders are subject to overlap by either the monotonic (IOR) or ramp components of the PSF.

In broad strokes, an initial estimate of the overlap for a given order is performed by computing peaks of adjacent orders above the interorder flux minimum and using the PSF to compute the fractional order flux to be subtracted from the sampled interorder fluxes. Before discussing this procedure in detail, it is necessary first to describe in more detail the different domains of a Pass 1 swath where each of the PSF components dominates.

#### A.2.2.2 Differentiation of Swath Regions

The continuous undulating line in Figure A.2 is the Chebyshev solution for an actual Pass 1 swath of an SWP image. The IOR area is denoted by a dashed triangle with vertices at spatial pixel numbers *nc*, *nf*, and *nd*. The normal execution of the background determination code requires that valid background pixels are sampled at these three points as well as the adjacent points $nc - 1$, $nf + 1$, and $nd + 1$. In Figure A.2 the rise from *nd* to *nf* is determined largely by the width of the PSF. This slope may vary because of circumstances for a particular exposure. For example, the slope of the $\overline{nf\ nd}$ leg of the IOR triangle is different for trailed images than for point-source images. Because this slope is a property of the swath itself, *BCKGRD* can use it to refine the overlap as estimated from the model PSF. The overlap between *nc* and *nf* depends primarily on source energy distribution and not exposure parameters. The effect of overlap near pixel *nc* appears to decrease in the figure, but this is an artifact of the rapidly decreasing camera sensitivity at short wavelengths.

#### A.2.2.3 Swath-Dependent Data Files

Default template files have been created that specify the spatial pixel numbers to be avoided in the Pass 1 background extraction for each camera and for all source types (point, extended, and noncontinuum) sources. The file also includes values for *nc*, *nf*, and *nd* of the IOR. Initially, the list of spatial positions to be avoided includes only the starting and ending values and the echelle order positions, but this is modified for a particular image in the initial *Data Screening* step (Section A.2.1) from the $\nu$ flags determined in the raw image screening (*RAW_SCREEN*) step.

#### A.2.2.4 On-the-Fly Pathology Screening

The fluxes on and off the echelle orders are used in Pass 1 to determine representative order heights and to estimate a PSF scaling factor unique to every swath of the image processed. Checks are made at this point to clip aberrant background flux values not flagged by *RAW_SCREEN* (e.g., from negative flux extrapolations or undetected cosmic rays). Anomalous interorder flux values in such cases are replaced with local means. The same procedure is repeated if necessary to substitute highly anomalous interorder fluxes with the means of the four neighboring interorder fluxes. This procedure was adopted to cope with small pixel clusters in the long-wavelength cameras that are prone to excessive negative extrapolations.

#### A.2.2.5 PSF Modeling

The estimate of the contamination of IOR and halation-ramp region fluxes by illumination from the spectral orders proceeds in two steps. Information from the PSF model and from the echelle order fluxes is not used in the first step, nor is a halation overlap region defined.

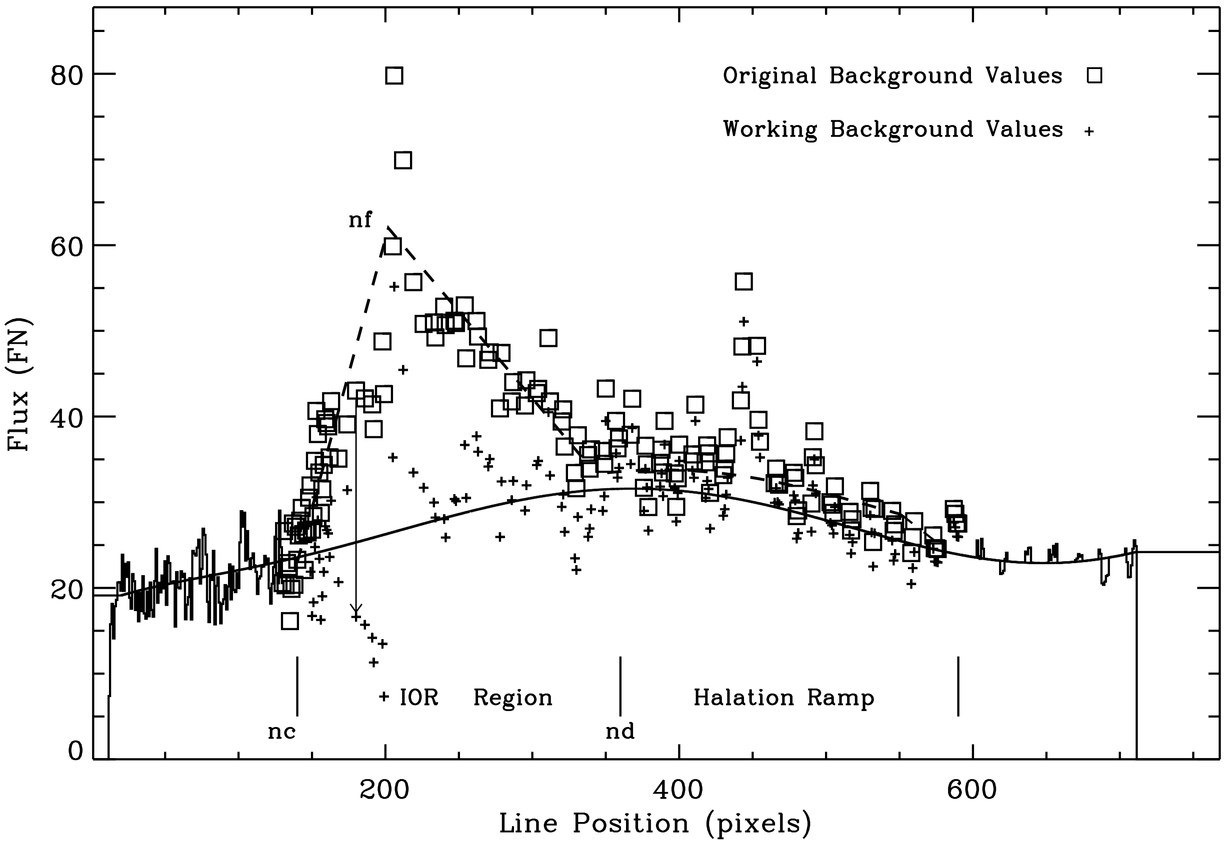


Figure A.2: Crosscut of background fluxes from a central "Pass 1" swath through an SWP image. Stellar fluxes are off-scale in this diagram. The triangular area describes the local raw background fluxes in the Interorder-Overlap Region where order crowding is severe; the halation region is shown to the right. Small crosses denote the raw fluxes corrected for overlap by the PSF model. The solid line is the Pass 1 solution, a Chebyshev, degree-7 polynomial.

The solution in this "Step 1" of Pass 1 is determined entirely from a Chebyshev interpolation from points in the end (non-IOR) regions of the swath. In the presence of certain image pathologies (Section A.2.4), as well as the first and last few Pass 1 swaths, this Step 1 is the only step; it becomes the final solution for the Pass 1 phase.

For the great majority of Pass 1 swaths, i.e. those passing through the middle of the camera image and not encountering poor statistical solutions, *BCKGRD* continues with a Step 2. This step uses the solution from Step 1 as a starting point to compute a PSF-compensated solution in which we attempt to subtract from the measured interorder fluxes the contamination from adjacent orders. As can be inferred from Figure A.3, the correction for this overlap can be determined by the simple relation:

$$Flux_{corr} = OrderHeight \; \times \; 2PSF_1/[1 - 2(PSF_1 - PSF_2)],$$

where $Flux_{corr}$ and $OrderHeight$ are given in FN flux units per pixel and $PSF_1$ and $PSF_2$ are given as a fraction of the *true* local order height. Step 2 concludes by subtracting $Flux_{corr}$ from the local measured background at each interorder location and refitting a new Chebyshev solution through the adjusted Pass 1 swath values. Note particularly that in NEWSIPS an explicit effort is made to compensate for the contamination of the it interorder fluxes (i.e., the background fluxes) in the manner described above, there is no adjustment made to correct the *on-order fluxes* (gross fluxes) for the effects of overlapping orders.

*BCKGRD* uses the same trial spatial PSF model for all types of continuum source types in a given camera. The algorithm also assumes that the PSF is global over the image. The model was determined by replicating the accumulation of flux overlap toward short wavelength orders from a large number of actual images.

Because the PSF may actually change from image to image, the algorithm attempts to accommodate such changes by using on-the-fly order information to refine the PSF model – specifically the slope of the $\overline{nf \; nd}$ leg of the IOR triangle. This is accomplished by comparing the fractional flux overlap with the model result for a reference order within the IOR, that is by comparing the increase in overlap for this order to the overlap found at the start of the IOR (pixel *nd*). If the measured and model slopes agree within a tolerance factor (1.5×), the program adopts the measured slope and scales the model PSF accordingly. Otherwise, the model PSF is used. Tests show that various Pass 1 swaths for a given image can either pass or fail this tolerance test independently.

#### A.2.2.6 Post-Solution Pathology Tests

After a continuous Chebyshev solution is computed for a particular Pass 1 swath, a series of data pathology checks are performed on the solution (see Section A.2.5). These tests are performed only on images of point and extended sources containing continuum flux. If the solution fails any of the pathology checks, an appropriate condition is relaxed (e.g. the PSF is not used to calculate the true interorder background, or the degree of the Chebyshev fit is decreased by one). The solution is then recalculated iteratively. Since even adjacent Pass 1 swaths sometimes can pass different pathology tests, their solutions can occasionally be different. This is a subtle but often important source of error in the final background solution. The results of these differing solutions are manifested as "spike structure" in Figure A.4, as described below.

### A.2.3 Pass 2: Dispersion Direction Swaths

In the second operation, Pass 2, inferred background fluxes at the order positions are sampled and assembled as arrays in the spectral direction. The fluxes from the Pass 1 solutions are used to compute a continuous Chebyshev solution for the background at each echelle order position. The generation of a fit along the positions of the echelle orders proceeds with the computation of a 7th-degree Chebyshev function interpolated for all sample (wavelength) positions. In this step it is not necessary to screen or exclude pixels or to test for data pathologies – only a single iteration is required. The Pass 2 operation tends to dilute the effects of poor solutions from a single Pass 1 swath. However, it also introduces a second smoothing into the final background surface.

Figure A.4 shows a final solution obtained for Order 95 of image SWP20931 on the B0 star HD93222. This order contains a strong Lyman-$\alpha$ feature. The spike pattern indicates samplings from the 26 swaths in Pass 1. A comparison of the residuals (comb pattern in the figure) shows that the solution for the Lyman-$\alpha$ order is less certain than those for long-wavelength orders where uncontaminated background pixels are common.

### A.2.4 Non-continuum images

The existence or absence of continuum flux in an *IUE* echellogram is determined by the order registration module. Because interorder-overlap flux can affect background determinations only for continuum images, in the noncontinuum case *BCKGRD* does not go through a Pass 1 step. The background estimates for these images are determined by sampling the interorder background on the long-wavelength side (spatial) of a given order with a one-pixel slit. A 7th degree Chebyshev solution is then computed for this nearly continuous array of interorder pixels. Note that tests show that some minor contamination from strongly saturated emission lines has been detected in neighboring orders.

### A.2.5 Data Pathology Assessments

Occasionally circumstances in the interorder fluxes lead to solutions that are slightly unstable, producing wiggles in an interpolated region that go beyond the flux range of sampled pixels at the two spatial ends of the camera. Such occurrences may be caused by abnormal conditions affecting the image (e.g. target-ring glow, cosmic ray hits, LWR flare, flux downturns at camera edge). A series of eight "pathology tests" has been added to *BCKGRD* to protect against blind solutions at the end of Pass 1 that do not agree with simple and often correct interpolations. These checks generally rely on a comparison of fluxes at two or more pixels along the swath or on a ratio of smoothed flux ranges. The rms statistic computed

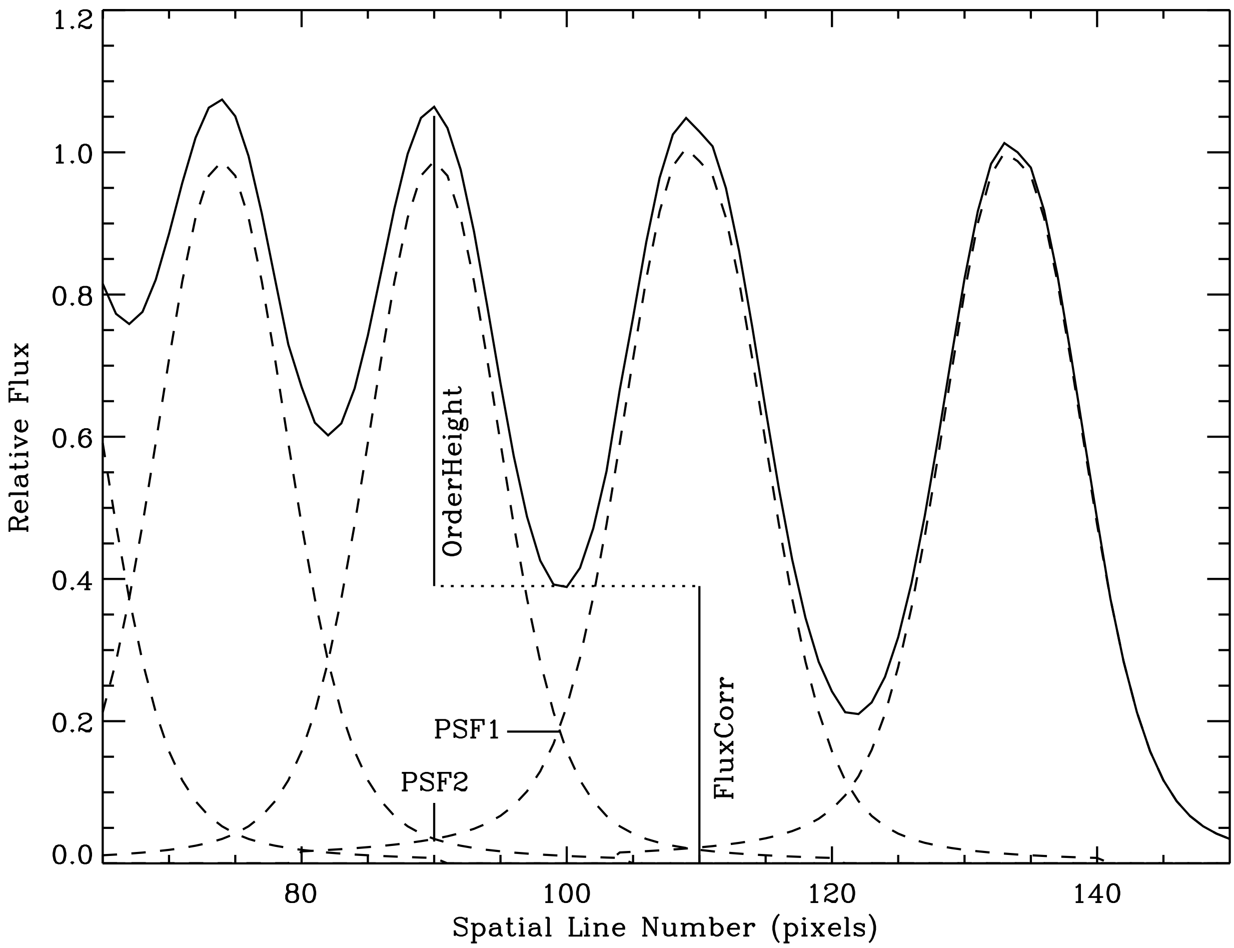


Figure A.3: A depiction of the influence of interorder overlap in progressively raising the intensity of (unit height) orders towards shorter wavelengths (left). The dashed lines represent intensities the orders would have if there were no overlap.

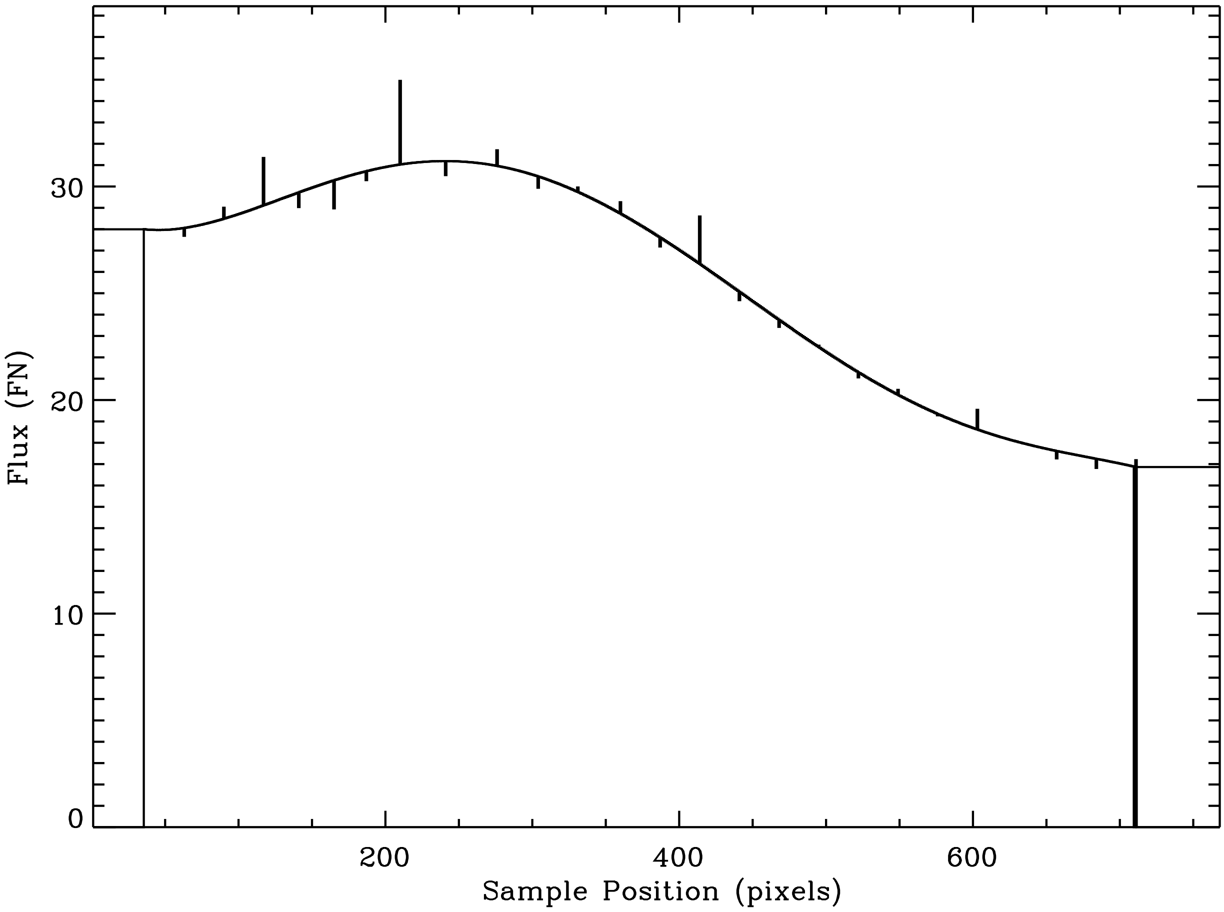


Figure A.4: Final background solution for SWP20931, order 95 (smooth solid line). The comb structure connected to the solution reflects the solutions for the various Pass 1 swaths sampled at the line position of this order.

from local raw background fluxes is a convenient unit of measure for flux ranges because it does not rely upon source brightness, exposure time, or an arbitrary flux level. In most cases a failure of a solution in a pathology test causes either the PSF information not to be used in Pass 1, the degree of the polynomial fit to the interorder data to be reduced, or both. Lowering the fitting degree has the effect of removing extra wiggles in the solution; however, the degree of the Chebyshev fit is never reduced below 3. In those cases where superfluous wiggles in the IOR region persist stubbornly after a few trials, a simple linear interpolation is adopted between "good" regions. This may occur for spatial positions toward the short wavelength (spatial) end of the IOR for certain swaths having reliable background samplings at the target edge. These tests are used only for continuum source images in Pass 1. Therefore, the final output background vectors from Pass 2 are still guaranteed to be pure continuous Chebyshev functions.

The data pathology tests keep track of the number of iterations through the swath-fitting routines, as well as a history of previous failure modes. Certain pathologies have been found to oscillate sometimes between two types of failures. If such patterns are detected, a fall-back exit option is adopted. Table refbtab1 summarizes the pathology checks and the strategies for circumventing them in subsequent iterations of the swath-fitting routine.

*BCKGRD* establishes a hierarchy of severity for the various pathologies it identifies. Tests 1–4 and 8 are the most critical, and the responses to failure of them are therefore more severe. Each test looks for a different and well known pathology. For example, Test 4 and Test 6 search for subtly different degrees of a similar pathology, so their response strategies are different. Test 2 searches for a solution minimum within the IOR (exceeding a tolerance) compared over the rest of the swath whereas Test 8 searches for a flux minimum in the solution anywhere within the swath. Test 2 permits a milder fix while Test 8 looks for a more severe IOR minimum. If Test 8 detects this condition, a linear interpolation between $nc$ and 50 pixels beyond $nd$ is used, with points in the halation ramp taken from the measured interorder flux values, without consideration of the PSF. If Test 2 repeatedly fails, the IOR-minimum pathology is guaranteed to be addressed by linear interpolation in Test 8.

Experience has shown that Test 7 is one of the most commonly occurring rejections of an initial solution. This test rejects having a local maximum at the high-sample number end of a swath. These rejections are often caused by an abnormal global shift of the spectral image format combined with target ring glow, but they can result also from any systematic rise in flux toward the short wavelength (spatial) end of the camera as well. If the pathology cannot be circumvented by decreasing the degree of the Chebyshev fit or by resorting to ignoring the PSF information in the swath-fitting routine, the solution is admitted. Test 7 is similar to Test 3 but checks for two maxima in the the middle of the short-wavelength (spatial) end of the image. In Test 3 one of the maxima searched for must be within the IOR, but this is not necessarily true for Test 7. Test 3 also checks for flare discharges which can occur in the long-wavelength corner of LWR images and computes two possible solutions: the first is a pure Chebyshev solution with the flare points deweighted and the second is a quadratic extrapolation of the solution without the flared region included. The solution with lower fluxes in the upturned flare region is then adopted, as this solution causes ringing less frequently.

A rejection by Test 5a, which searches for a maximum in the IOR, causes the degree of the fit to be decreased on the first iteration and halves the trial PSF slope factor. It interpolates linearly over this region if additional iterations are necessary. Test 5b searches for an excessive minimum for spatial positions at the short wavelength (spatial) end of the image and the beginning of the IOR. A minimum in the IOR is usually caused either by a bright target ring at the beginning of the swath, or an overestimate of the PSF. Such conditions cause a false overcorrection for background contamination within the IOR and hence a background solution which is too low. Both tests are addressed by decreasing the Chebyshev degree.

## A.3 Failure Modes

The background swath fitting process is considered to fail a particular Pass 1 swath if any of the following conditions apply.

- Fewer than 20 valid background pixels exist in the swath.
- The first two valid background pixels in the swath are not continuous.
- There are no data gaps in the swath (continuum image only).
- The starting pixel for the IOR is less than spatial pixel number 3 in the swath (continuum sources only).
- The first and last pixel with usable background fluxes are on the same side of the IOR (continuum sources only).

When a solution for a Pass 1 swath fails any of these tests, the background solution is set to zero for the entire swath. If this occurs for an isolated swath, an interpolated solution based on the two neighboring Pass 1 swaths is substituted for the original solution. If two consecutive Pass 1 swaths, or a total of five, have null values based on these conditions, the background arrays for the entire image are set to zero, and *BCKGRD* has “given up” on the image. This occurs for an exceedingly small number of images (e.g., about 13 out of 12,898 images in the GSFC high-dispersion archives), usually as a consequence of a major portion of the image being missing. This condition is documented in the processing history log.

## A.4 Problem Areas

Tests have shown that high-dispersion spectra from each of the three *IUE* cameras have characteristics that impose unique challenges for automated background extraction algorithms. The great diversity of image types in the archives prohibits implementing any strategy that

Table A.1: Recourses to Various Pathological Trial Solutions

| TEST NUMBER | CONDITION/RECOURSES |
| --- | --- |
| 1<br>Short Swaths | Solution monotonic between *nd* & *nf*:<br>If poly. degree $>3$, decrease degree;<br>otherwise linearly interpolate. |
| 2<br>IOR Min. | Min. in IOR between *nc* & *nd*;<br>decrease degree,<br>on third attempt, give up. |
| 3<br>Max. near swath end<br>[LWR Flare] | Max. at high sample no.:<br>decrease degree.<br>[Lower weights for points in flare] |
| 4<br>IOR Max. | Max. in IOR is max. for swath:<br>decrease degree |
| 5a<br>Max. at or near swath start | Max. at low sample no.:<br>decrease degree & reduce<br>slope of PSF model |
| 5b<br>Min. at or near swath start | Min. at low sample no.:<br>1st time: go to Test 6;<br>thereafter: decrease degree or<br>interpolate linear solution |
| 6<br>IOR max. | Max. within IOR:<br>decrease degree or<br>interpolate linearly across IOR |
| 7<br>Max. at end | Max. at high sample no.:<br>decrease degree |
| 8<br>IOR min.<br>Absolute! | Absolute min. is in IOR:<br>interpolate linearly in IOR |

makes assumptions about the behavior of source spectra in order to fix background problems, particularly in an automated processing environment.

The SWP camera has a unique confluence of conditions, a circular target ring and a blaze function shifted towards short wavelengths along the echelle-dispersion direction, which together make it impossible to sample local background at the short wavelength corner of the image. For spectra of early-type objects, these conditions almost guarantee that for the shortest-wavelength swaths in Pass 1 no pixels will be found at the short end (spatial) of the swath to use for interpolation in the IOR. In these cases the solutions will turn upwards in this region. This problem is addressed at the end of the first pass of *BCKGRD* by grafting a solution from a neighboring swath in place of the turned-up solution. Experience shows that this strategy is sometimes only partially successful for SWP images. As a result the final background solution in the short-wavelength corner is sometimes too high. This behavior can influence the background solutions for the blue wing of Lyman $\alpha$ and lines of neighboring echelle orders that fall in the same blaze region to be as much as a few percent too high relative to the local continuum. This is probably the most significant systematic error produced by *BCKGRD*. However, we emphasize that this problem is inherent in the placement of these spectral features close to the target ring. Therefore, even customized extractions will not be able to model an accurate local background solution in this region.

Both long-wavelength cameras have the problem of a number of specific pixels being habitually converted from low DNs to highly negative FNs. In general, this is not a problem because *BCKGRD* clips highly aberrant fluxes before its Chebyshev fitting. However, the problem of clipping only aberrant fluxes is complicated for the LWP camera because of the turndown of the local background at the long-wavelength (spatial) end of the target. This complexity has been treated by disallowing clipping of anomalous fluxes in this region of the LWP image. Another complication is that although a 7th degree is usually sufficient to fit the flux turndown near the target ring, the solution may not adequately follow the turndown if the background fluxes are noisy or have caused the Chebyshev degree to be reduced to less than 6. Generally, there are no "notable" spectral lines in these orders, but a customized extraction can take care of this problem should the need arise.

An additional characteristic of the LWP camera fluxes is the abrupt increase in noise in the short (spatial) end of the image. It is not clear that this causes systematic background deviations, but it may cause a degraded accuracy in the background result.

The LWR camera exhibits a few patches of enhanced sensitivity that are not completely calibrated out in the photometric correction step. The most dramatic of these is the "flare" at the long spatial and short-wavelength (dispersion) corner of late-epoch images. Inspection of many images shows an upturn in the local background in this area even during the *IUE* Commissioning Period. Therefore, background fluxes extracted in this area either by NEWSIPS or by customized extractions should be used with caution.